Int J Clin Exp Pathol 2026;19(6):248-260
www.ijcep.com /ISSN:1936-2625/IJCEP0170219

Original Article

TMEM161B-AS1: a pivotal long non-coding RNA in the pathogenesis of glioblastoma revealed by Mendelian randomization analysis

Ya-Li Yan[1], Jia-Wei Zhang[3], Bin Liu[2], Peng Bai[2], Jin Zhen[2], Shi-Chao Wang[3]

[1]Ministry of Scientific Research, The First Hospital of Hohhot, Hohhot 010018, Inner Mongolia, China; [2]Department of Neurology, The People's Hospital of Inner Mongolia, Hohhot 010018, Inner Mongolia, China; [3]The Clinical Genetic Laboratory, The First Hospital of Hohhot, Hohhot 010018, Inner Mongolia, China

Received November 23, 2025; Accepted March 6, 2026; Epub June 15, 2026; Published June 30, 2026

Abstract: Objectives: The significance of long non-coding RNAs (lncRNAs) in glioblastoma multiforme (GBM) has been acknowledged, but their specific role in the pathogenesis of GBM has not been thoroughly investigatedr. This study aimed to investigate the involvement of lncRNAs in the pathogenesis of GBM. Methods: We collected GBM tissues from four patients and corresponding para-carcinoma controls samples, and used HiSeq sequencing to generate lncRNA expression profiles in GBM. To identify lncRNAs associated with GBM, we employed Mendelian randomization (MR), leveraging the comprehensive extensive expression data obtained from HiSeq sequencing to infer causal relationships. Expression quantitative trait loci (eQTLs) for brain tissues were accessed from the Genotype-Tissue Expression (GTEx) Portal. Subsequently, we conducted an integrative analysis combining brain cancer genome-wide association study (GWAS) summary data (finn-b-C3_GBM) with eQTL data using MR. Differentially expressed lncRNAs were intersected with MR results to identify lncRNA candidates. Subsequently, the ENCORI database was used to identify genes regulated by the candidate lncRNAs, and Gene Ontology and Kyoto Encyclopedia of Genes and Genomes pathway enrichment analyses were performed. Result: A protein-protein interaction (PPI) network was constructed to identify hub genes associated with GBM, and these findings were validated using the Gene Expression Profiling Interactive Analysis 2 (GEPIA2) tool. A total of 106 lncRNAs exhibited significant alterations in expression levels ($|\log_2(\text{fold change})| > 1$ and $P < 0.05$) in GBM tissues. Through Mendelian randomization (MR) analysis, TMEM161B-AS1 emerged as a promising candidate lncRNA. Genes regulated by TMEM161B-AS1 were significantly enriched in biological processes such as DNA replication and repair, cellular response to DNA damage stimuli, and pathways including the peroxisome proliferator-activated receptor signaling pathway, nucleotide excision repair, and the Fanconi anemia pathway. The differential expression of hub genes CUL4A, RPA1, and BRIP1 was validated using the GEPIA2 database. Conclusions: These findings suggest pathways for the development of more precise and sensitive biomarkers for the diagnosis and management of GBM, which may ultimately enhance patient outcomes.

Keywords: Glioblastoma multiforme, lncRNA expression profiles, Mendelian randomization, TMEM161B-AS1

Introduction

Glioblastoma multiforme (GBM) is a common and highly malignant primary brain tumor, characterized by its aggressive infiltrative behavior and potential for extracranial dissemination [1]. The standard therapeutic approach for GBM typically involves surgical resection followed by adjuvant radiotherapy and chemotherapy. However, achieving a gross total resection (GTR) of gliomas exceeding 90% remains a significant challenge, and incomplete excision often leads to disease recurrence. Approximately 10% of GBM cases exhibit a lower recurrence rate, while some gliomas manifest malignant transformation upon recurrence [2]. Despite advancements in surgical technique, radiotherapy, and medical care, the overall survival rate for GBM patients has shown limited improvement [3]. Chemotherapy, although a well-established therapeutic approach, has its limitations, with a median overall survival rate ranging from 14.5 to 16.6 months [3, 4]. The poor prognosis associated with GBM is attributed to factors such as

https://doi.org/10.62347/ATCH1081

tumor heterogeneity, rapid cellular proliferation, and extensive invasion. Additionally, the lack of a comprehensive understanding of the molecular mechanisms underlying GBM and the absence of clearly defined therapeutic targets further complicate effective treatment. Furthermore, the limited understanding of the molecular mechanisms underlying GBM and the absence of a comprehensive framework for treatment continue to impede significant progress in patient outcome.

Long non-coding RNAs (lncRNAs) represent a category of non-coding RNAs that, although not involved in protein coding, are integral to the regulation of various biologic processes. These lncRNAs have been shown to play crucial roles in key cellular events, such as epigenetic regulation, cell cycle progression, and cellular differentiation [5-7]. Moreover, dysregulation of lncRNA expression in clinical samples has been associated with tumor malignancy and histologic subtype, suggesting their use as biomarkers for glioma and their relevance for therapeutic strategies [8]. The intercellular transfer of lncRNAs also plays a significant role in intercellular signaling, contributing to the maintenance of the tumor microenvironment and possibly facilitating tumor metastasis [9]. Despite their potential importance, there is little research focused on elucidating the specific functions of lncRNAs in gliomas.

Among the long non-coding RNAs (lncRNAs) associated with glioblastoma (GBM), TMEM161B-AS1 has emerged as a significant factor. Recent research has demonstrated that TMEM161B-AS1 is involved in various biologic processes pertinent to cancer progression. For example, in esophageal squamous cell carcinoma, TMEM161B-AS1 functions as a suppressor of cell proliferation, invasion, and glycolysis by interacting with the miR-23a-3p/HIF1AN signaling pathway, suggesting a potential tumor-suppressive role [10]. In contrast, in oral squamous cell carcinoma, particularly in individuals infected with human papillomavirus (HPV), TMEM161B-AS1 is markedly upregulated and correlates with adverse clinical outcome, indicating a tumor-promoting role in this context [11].

In the context of glioblastoma multiforme (GBM), TMEM161B-AS1 has been implicated in facilitating malignant phenotypes in glioma cells, including resistance to the chemotherapeutic agent temozolomide (TMZ). This occurs through the sequestration of hsa-miR-27a-3p, leading to the upregulation of several ferroptosis-related genes [10]. These observations collectively indicate that TMEM161B-AS1 plays a complex role in the pathogenesis of GBM, exhibiting both tumor-suppressive and oncogenic functions contingent upon the cellular environment. Given the limited understanding of glioma biology and the urgent demand for more effective therapeutic intervention, it is crucial to investigate the molecular pathways underlying GBM development and progression, particularly those involving long non-coding RNAs (lncRNAs) such as TMEM161B-AS1.

Mendelian randomization (MR) is a prevalent methodology for inferring causal relationships between traits and diseases, leveraging the stable inheritance patterns of genetic variants to establish clear causal sequences. This approach is regarded as one of the most reliable techniques for causal inference, second only to randomized controlled trials. By integrating data from expression quantitative trait loci (eQTL) and genome-wide association studies (GWAS), MR has proven effective in identifying pleiotropic associations between gene expression and various traits [10]. The primary aim of this study is to investigate the role of GBM-associated lncRNAs in the pathogenesis of GBM. To achieve this, we conduct an MR study to identify the key lncRNAs involved in the development and progression of GBM.

Materials and methods

Study design

Figure 1 illustrates the method employed in this study. RNA sequencing (RNA-seq) was used to analyze the expression profiles of lncRNAs in glioma patients, with subsequent validation of lncRNA expression through database mining. MR analysis was employed to identify lncRNAs associated with GBM, and their target mRNAs were predicted using the ENCORI database. Gene Ontology (GO) and Kyoto Encyclopedia of Genes and Genomes (KEGG) pathway enrichment analyses were conducted to explore the potential functions of genes regulated by lncRNA identified through MR analysis. Additionally, a Protein-Protein Interaction (PPI) network was constructed to identify hub genes.

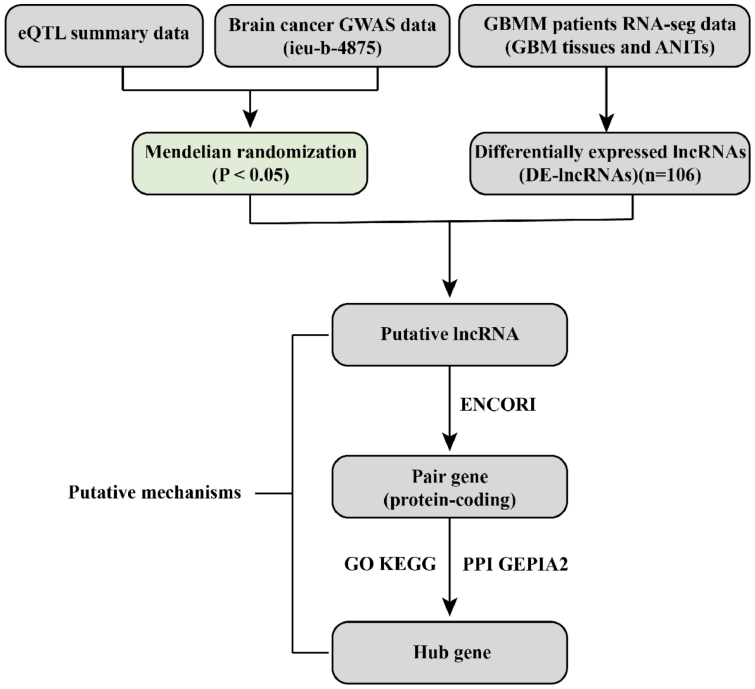

Figure 1. Workflow of the study.

Table 1. Patients' clinical characteristics

	GBM	ANIT
Number (n)	4	4
Age (years)	35-60	35-60
Sex (male/female)	4	4
TNM stage	IV	/
Histologic type	Frontal lobe (n = 3)	Frontal lobe (n = 3)
Label	AT	AC
	BT	BC
	CT	CC
	DT	DC

Clinical sample collection

All GBM tissues were collected from Hohhot First Hospital and Inner Mongolia People's Hospital in Inner Mongolia, China. The study criteria adhered strictly to the guidelines established in China for the diagnosis and treatment of GBM in the central nervous system (CNS) and the CNS tumor classifications outlined by the World Health Organization [11]. Samples of the GBM focal zone and adjacent non-involved tissue (ANIT) were collected from patients in stages III-IV, aged between 35-60 years. The ANIT samples were obtained at a distance from the tumor margins. The GBM and ANIT specimens were evaluated using histopathologic methods in the Department of Pathology and staged according to the TNM classification system. Sample details were provided in **Table 1**. The TNM staging system is used worldwide as a benchmark for staging cancers; it considers the weight and category of the tumor, as well as multiple distant metastases [12]. All lesions were in the cerebral hemispheres; three were in the frontal lobe and one in the temporal lobe.

Sequencing library preparation and data analysis

RNA was prepared from 5 μg of total RNA per sample. NEBNext® Ultra™ Directional RNA Library Prep Kit for Illumina® (New England Biolabs [NEB], Ipswich, MA, USA) was used to prepare the sequencing libraries. A 150-200 base pair (bp) cDNA was selected using Beckman Coulter's AMPure XP system (Brea, CA, USA). The PCR was performed with Phusion High-Fidelity DNA polymerase, universal PCR primers, and Index (X) Primer (NEB). Finally, the products were purified using the AMPure XP system and library quality was assessed by the Bioanalyzer 2100 system (Agilent, Santa Clara, CA, USA). In order to cluster the index-coded samples, a cBot Cluster Generation System was used. The TruSeq PE Cluster Kit v3-cBot-HS (Illumina, San Diego, CA, USA) was used according to the manufacturer's instructions. Clusters generated from the libraries were sequenced on the Illumina Hiseq 4000 platform and 150 bp paired-end reads were generated. Raw data (raw reads) in fastq format were processed using in-house Perl scripts. All of the following analyses were conducted using high-quality clean data. The reference genome and gene model annotation files were downloaded from the genome website. The reference genome

index was built using Bowtie2 v2.2.8, and paired-end clean reads were aligned to the reference genome using Bowtie [3]. To identify the most promising and suitable lncRNAs, we applied the following criteria: $|\log_2(\text{Fold Change})| > 1$ and $P < 0.05$; lncRNA lengths ranging from 500-3000 nucleotides; and the presence of potentially GBM-related genes within a 100 kilobase region.

Data source and Mendelian randomization (MR)

Experimental validation is a rigorous yet labor-intensive process that enhances the robustness of evidence. In contrast, MR leverages genetic variation to simulate the effects of randomized experiments, facilitating causal inference [13]. In order to provide genetic evidence, a MR analysis was conducted to determine causal relationships between lncRNAs and GBM. Cis-eQTLs from 13 brain tissues from GTEx release v8 were utilized in the present study. Summary statistics for all variant-gene eQTL pairs tested in each of the brain tissues, the significant Genes and Variants at FDR < 0.05, and the gene expression levels and LeafCutter95 values can be accessed for download from the GTEx portal (https://gtexportal.org/home/datasets) [14]. Summary-level data related to GBM were sourced from the FinnGen biobank, which involved a sample size of 208,792 individuals (ncase = 91, ncontrol = 218,701) of European descent and encompassed 16,380,466 single nucleotide polymorphisms (SNPs). The summary data can be downloaded from Medical Research Council Integrated Epidemiology Unit (MRC-IEU) project (GWAS ID: finn-b-C3_GBM). Following data collection, analysis was conducted using MR, which involved the removal of linkage disequilibrium (LD), weak instrumental variables (IVs), and confounders using the R package TwoSampleMR (v0.5.6) and MendelianRandomization (v0.8.0). The effect of each instrumental variable on the outcome was assessed by using the Wald ratio [15]. In order to estimate the causal effects, a random-effects inverse variance-weighted (IVW) meta-analysis of each Wald ratio was predominantly used along with four additional methods (MR Egger, Weighted Median, Simple Median, and Weighted Mode). The heterogeneity of causal effects among IVs was assessed using Cochran's Q statistic, and funnel plots were employed to detect any presence of heterogeneity through asymmetry. Directional horizontal pleiotropy was evaluated using MR-Egger regression [16].

Functional prediction analysis of candidate lncRNA

We obtained the candidate lncRNA by taking the intersection of the differentially expressed lncRNAs (DE lncRNAs) and MR results. To elucidate the role of the candidate lncRNA, the ENCORI database (https://rnasysu.com/encori/) was used to predict protein-coding mRNAs that are potentially regulated by the lncRNA and are causally linked to GBM [17]. Subsequently, GO and KEGG pathway enrichment analyses were conducted on the identified mRNAs using the Database for Annotation, Visualization, and Integrated Discovery (DAVID) (v6.8) (https://david.ncifcrf). The results of the enrichment analyses were visualized using R (4.3.0).

Protein-Protein Interaction (PPI) network construction and hub genes screening

The PPI network was constructed using the online tool STRING, (https://cn.string-db.org) [18]. The minimum required interaction score was set to 0.400, and disconnected nodes were excluded from the network. The resulting PPI network was imported into Cytoscape software (version 3.6.0) for visualization and further analysis Hub genes within the PPI network were identified using the cytoHubba plugin in Cytoscape [19]. The Degree algorithm was employed to calculate the connectivity of each node, and the top 10 genes were selected as hub genes based on their degree centrality ranking. The degree of a node represents the number of edges connected to it, reflecting its importance in the network. The gene expression levels of the screened hub genes in GBM were validated using the web-based tool GEPIA2 (http://gepia2.cancer-pku.cn/#index), with $|\log_2(\text{fold change})| > 1$ and $P < 0.05$ considered significant.

Statistical analysis

All statistical analyses were performed using R software (version 4.3.0). Differential expression analysis of lncRNAs: the DESeq2 package was used to identify differentially expressed lncRNAs between GBM tissues and adjacent non-involved tissues. The significance threshold was set at $|\log_2(\text{fold change})| > 1$ and

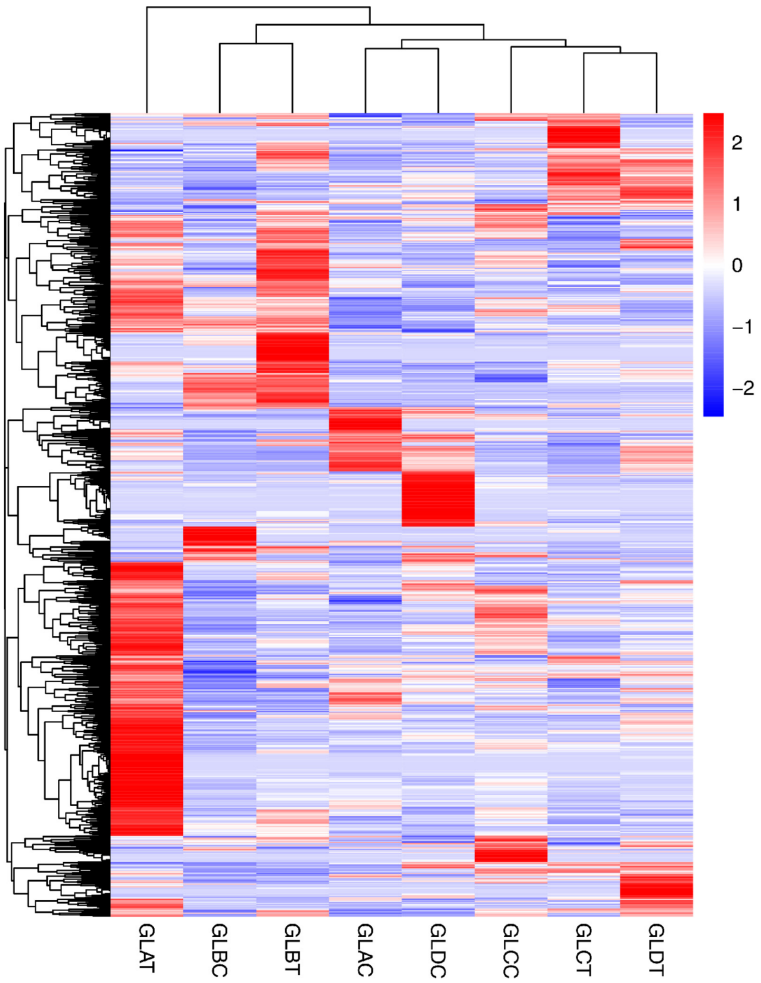

Figure 2. Heatmap and hierarchical clustering of lncRNA profile comparisons between GBM tissues and control. Each bar in the figure represents the trend of genes in the sample. Red indicates up-regulation; blue indicates down-regulation.

adjusted *P*-value < 0.05, with the Benjamini-Hochberg method applied for multiple testing correction.

Mendelian randomization analysis: the random-effects inverse variance-weighted (IVW) method was used as the primary approach to estimate causal effects. Four additional methods were employed for sensitivity analyses: MR-Egger regression, weighted median, simple median, and weighted mode. Heterogeneity among instrumental variables was assessed using Cochran's Q statistic, with P < 0.05 indicating significant heterogeneity. Horizontal pleiotropy was evaluated using the MR-Egger intercept test, where a *P*-value < 0.05 suggests the presence of directional pleiotropy. Leave-one-out analysis was performed to assess the robustness of the results by sequentially removing each SNP and recalculating the causal estimate. All MR analyses were conducted using the TwoSampleMR (version 0.5.6) and MendelianRandomization (version 0.8.0) R packages.

Gene Ontology (GO) and Kyoto Encyclopedia of Genes and Genomes (KEGG) pathway enrichment analyses: Fisher's exact test was used to determine the significance of enrichment, with the Benjamini-Hochberg method applied for multiple testing correction. Terms with adjusted *P*-value < 0.05 were considered significantly enriched.

Validation of hub gene expression using the GEPIA2 database, one-way ANOVA was used to compare gene expression levels between GBM tissues and normal tissues. A $|\log_2(\text{fold change})| > 1$ and *P*-value < 0.05 were considered significant.

Results

LncRNA expression profiles

The clinical profile of participants included in this research was documented in **Table 1**. A total of 106 lncRNAs demonstrated significant expression levels, with a $|\log_2(\text{Fold Change})| > 1$. The lncRNAs exhibiting differential expression were detailed in Table S1. Among the 106 lncRNAs, 52 showed upregulation while 54 showed downregulation in patients with GBM compared to the control cohort. The heatmaps illustrating the expression profiles of lncRNAs in both GBM and control subjects are depicted in **Figure 2**.

Mendelian randomization (MR) analysis

In this study, MR to investigate was used to explore the potential regulatory role of lncRNAs in the pathogenesis of GBM. The MR analysis identified a convergence with the DE lncRNAs, revealing three potential candidate lncRNAs (GUSBP11, LINC-0088, TMEM161B-AS1, Table

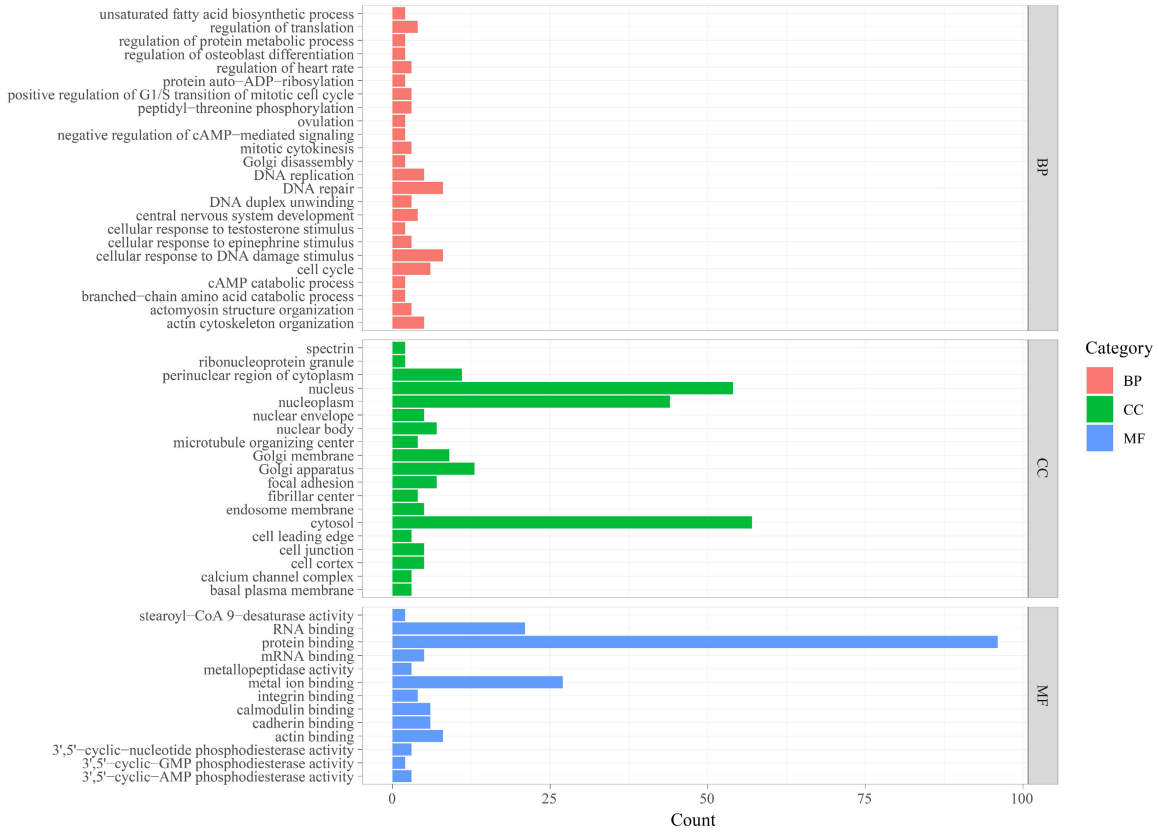

Figure 3. GO enrichment of TMEM161B-AS1 regulated genes.

S2, Figure S1) as implicated in the pathogenesis and progression of various cancers [20-22] Following the initial analysis, sensitivity analyses were conducted to evaluate the dependability of the findings. The application of Cochran's Q statistic (Table S3) revealed that there was no heterogeneity among SNPs in the MR analysis. Additionally, the MR-Egger intercept indicated the absence of directional pleiotropy (Table S4; Figure S2). The leave-one-out analysis revealed that the outcomes exhibited a high degree of robustness in terms of causality (Figure S3). Even when any of the SNPs were eliminated, the observed causal effects remained largely unaffected. These findings served as evidence for the reliability of the MR analysis. Notably, TMEM161B-AS1 has been associated with the malignant cytologic features of GBM [20]. Subsequently, our functional prediction analyses were focused specifically on TMEM161B-AS1.

GO and KEGG pathway analysis of predicted mRNAs

The genes regulated by TMEM161B-AS1, as predicted by ENCORI, are presented in Table S5. A comprehensive analysis of the 137 mRNAs revealed 57 Go terms associated with the predicted mRNAs, with a particular emphasis on biological processes. The role of these genes in the pathogenesis of GBM was illustrated in **Figure 3**, where they were found to be engaged in various processes such as DNA replication and repair, cellular response to DNA damage stimulus, and cell cycle, pathway analysis (**Figure 4**) indicated enrichment of 9 pathways in the predicted genes, including the PPAR signaling pathway, oxytocin signaling pathway, Renin secretion, nucleotide excision repair, and Fanconi anemia pathway.

PPI network construction and identification of Hub genes

A PPI network was constructed utilizing the STRING online database, with the inbuilt plugin cytoHubba of Cytoscape utilized for further screening of hub genes. The top 10 genes were selected based on their degree ranking, as illustrated in **Figure 5**. Among these, CUL4A, RPA1, and BRIP1 were identified as hub genes. The expression levels of these three hub genes

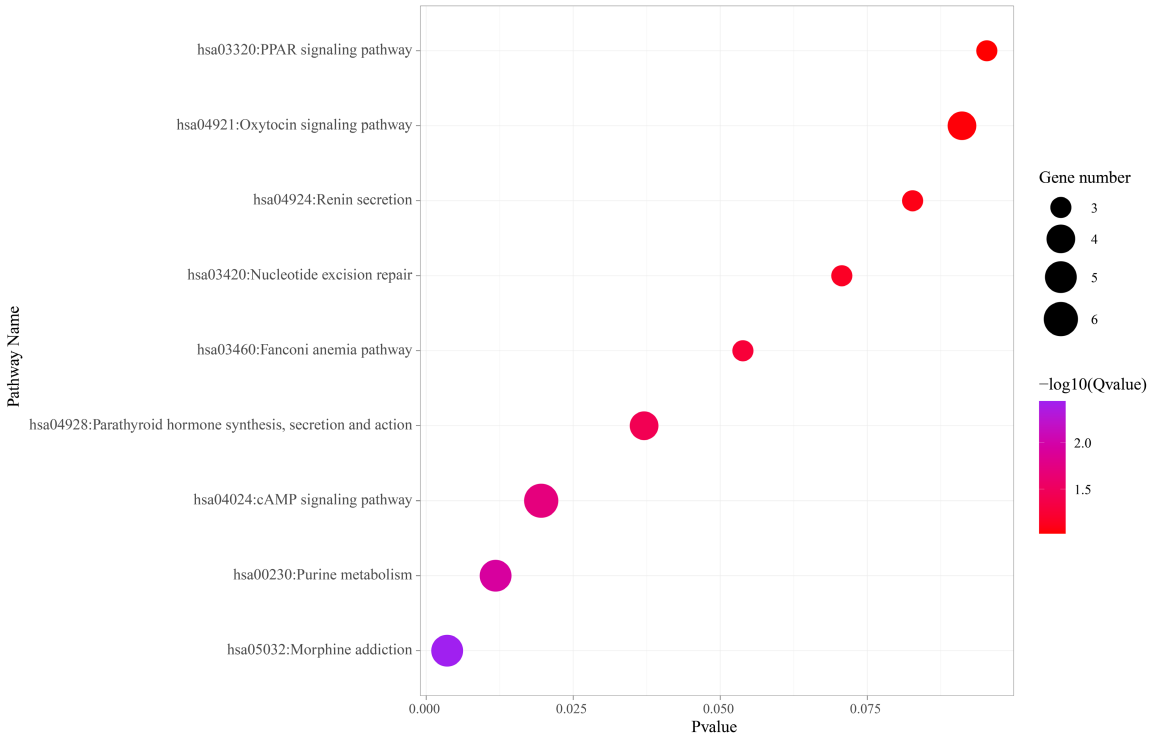

Figure 4. KEGG pathway enrichment of TMEM161B-AS1 regulated genes.

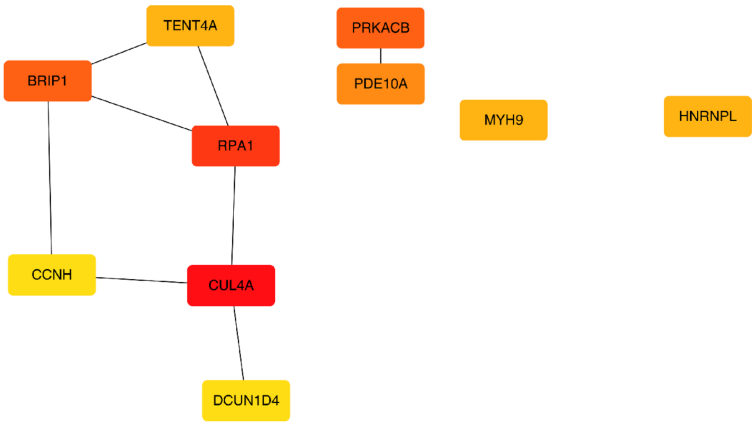

Figure 5. Protein-protein interaction of top 10 genes. Darker color indicates a prominent core position in the network.

in GBM were validated using the GEPIA2 database (**Figure 6**), which demonstrated significant differential expression in GBM tissue compared to normal tissue. To further elucidate the pathways associated with TMEM161B-AS1 **Figure 7** illustrates the biological relationships of the key genes and pathways that it governs.

Discussion

Glioma, recognized as the most prevalent and aggressive type of malignant brain tumor, poses significant challenges concerning treatment modalities and patient prognosis. The use of upstream therapy, which emphasizes the identification of biomarkers to mitigate the risk or progression of GBM, shows promise as a primary preventative approach against GBM. Nevertheless, the efficacy of upstream therapy is dependent on a comprehensive understanding of the intricate mechanisms underlying GBM pathogenesis.

In this study, we combined RNA sequencing of clinical GBM samples with Mendelian randomization analysis to screen for lncRNAs that may have causal roles in GBM pathogenesis. Among the 106 differentially expressed lncRNAs identified by RNA-seq, only TMEM161B-AS1 showed consistent causal association with GBM when we validated the results through MR analysis. By integrating expression data with genetic evidence, this approach offers a stronger basis for pinpointing lncRNA targets with therapeutic potential compared to using either method on its own.

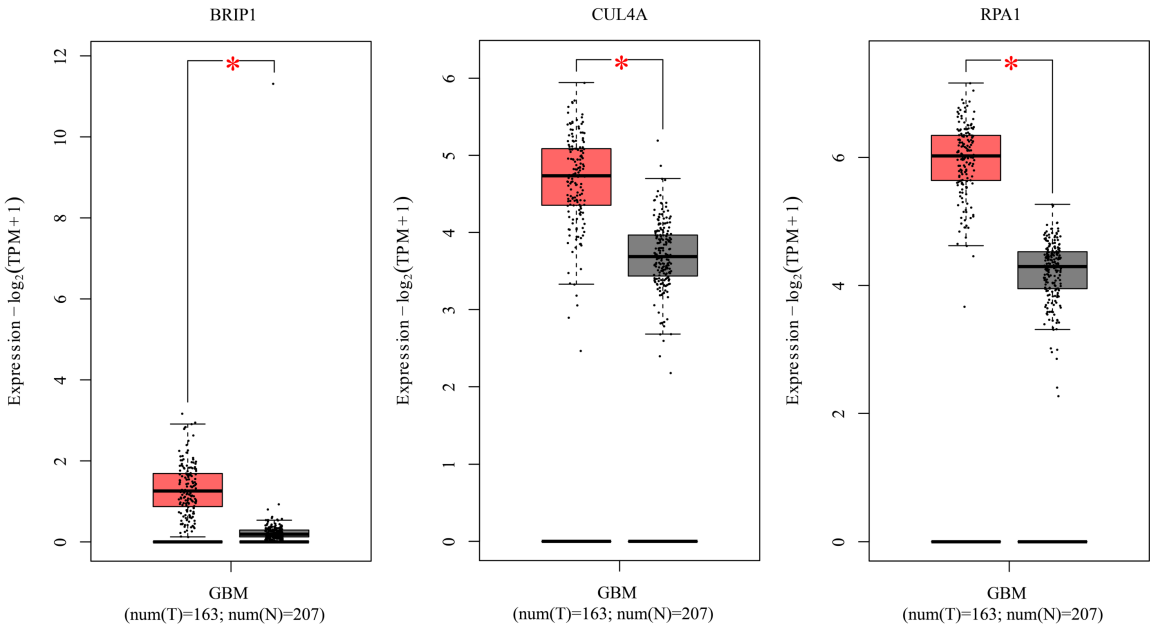

Figure 6. Expression of CUL4A, RPA1, and BRIP1 in GBM.

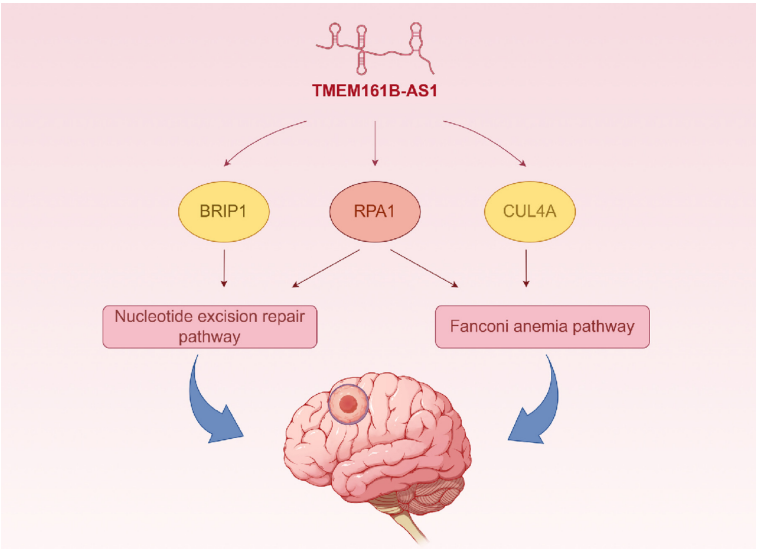

Figure 7. Key genes and pathways implicated in TMEM161B-AS1.

Non-coding RNAs (ncRNAs), once thought to be mere 'junk' DNA, have gained recognition for their significant contributions to the regulation of gene expression, cellular processes, and their implication in tumorigenesis [21, 22]. Recent research has concentrated on the pathological roles of ncRNAs in brain cancer, highlighting their potential as diagnostic biomarkers and therapeutic targets. Specifically, long non-coding RNAs (lncRNAs) such as H19 [23], BCYRN1 [24], NEAT1 [25], SNHG16 [26], and DLGAP1-AS2 [27] have been identified as significant contributors to either the inhibition or promotion of glioblastoma (GBM) tumorigenesis. Our findings indicate distinct expression patterns of certain lncRNAs, such as RP11, which align with existing literature identifying them as biomarkers and therapeutic targets in GBM [28]. *In vitro* experiments have demonstrated that the knockdown of RP11 suppresses various malignant glioma phenotypes, including cell proliferation, migration, invasion, and self-renewal capacity. Furthermore, RP11 has been shown to be activated by competitively sponging miR-1273g-3p [29]. Angiogenesis, a hallmark of cancer, is essential for glioma progression, and the vascular endothelial growth factor (VEGF) pathway has emerged as a prominent therapeutic target.

Given the limited information provided by Hiseq-sequencing, a MR analysis was conducted to identify the putative causal effects of lncRNA in GBM. The results of the analysis identified TMEM161B-AS1 (Transmembrane Protein

161B Antisense RNA 1) as putative causal lncRNA in GBM, indicating its significant role within the intricate network of non-coding RNAs that regulate various biological processes. Research has shown that the role for TMEM161B-AS1 in GBM is multifaceted, encompassing both tumor-suppressive and oncogenic functions. In the context of esophageal squamous cell carcinoma, TMEM161B-AS1 has been identified as a suppressor of proliferation, invasion, and glycolysis through its interaction with the miR-23a-3p/HIF1AN signaling pathway, indicating a potential tumor-suppressive function in this malignancy [23]. Conversely, in oral squamous cell carcinoma, particularly among individuals with human papillomavirus (HPV) infection, TMEM161B-AS1 exhibits significant upregulation and is associated with unfavorable clinical outcomes. Its role as a tumor promoter in this setting is attributed to its modulation of the miR-651-5p/BDNF axis, thereby influencing cell progression [24]. Based on MR analysis, we propose that TMEM161B-AS1 acts mainly as an oncogenic lncRNA in GBM. The positive causal effect from MR (OR > 1) points to elevated TMEM161B-AS1 expression as a potential contributor to GBM development. This interpretation fits better with the oncogenic role seen in oral squamous cell carcinoma than with the tumor-suppressive function reported in esophageal cancer, which suggests that TMEM161B-AS1 may behave differently depending on tissue type and cellular context. The unique features of the central nervous system microenvironment, such as the blood-brain barrier and its distinct immune characteristics, could be factors that shape how TMEM161B-AS1 carries out its regulatory functions in GBM.

Furthermore, TMEM161B-AS1 has been identified as a cellular senescence-related lncRNA with prognostic implications in patients with multiple myeloma, suggesting its involvement in cellular senescence processes [25]. Most importantly, TMEM161B-AS1 has been linked to promoting malignant behaviors in glioma cells, such as resistance to the chemotherapy drug temozolomide (TMZ), This resistance is mediated through the sequestration of hsa-miR-27a-3p, leading to the upregulation of several ferroptosis-related genes. These observations suggest that TMEM161B-AS1 contributes to cancer pathogenesis across various contexts [20]. However, further validation studies are necessary to delineate its specific functions and assess its use as a therapeutic target.

To elucidate the molecular mechanisms underlying the participation of TMEM161B-AS1 in the pathogenesis of GBM, we employed ENCORI to predict the coding-mRNAs regulated by TMEM161B-AS1, which were enriched in the PPAR signaling pathway, cAMP signaling pathway, and others. Previous studies have demonstrated the intricate roles of the three subtypes of peroxisome proliferator-activated receptors (PPAR) in various tumors, with research indicating that the inhibition of PGBD5 suppresses the malignant progression of glioma by enhancing the PPAR pathway [26]. Furthermore, the cAMP signaling pathway has been identified as a crucial pathway in the progression of GBM [27, 28]. The pathway enrichment analysis points to TMEM161B-AS1 as a potential hub that links several oncogenic signaling cascades in GBM. What caught our attention was the co-enrichment of both PPAR and cAMP pathways among genes regulated by TMEM161B-AS1, given that these two pathways are known to cross-talk during metabolic reprogramming in cancer cells. We think TMEM161B-AS1 may help GBM cells adapt their metabolism by modulating these interconnected pathways at the same time, which could support tumor cell survival and growth when nutrients are scarce in the tumor microenvironment.

In addition to the common signaling pathways above, our analysis of the predicted results suggests that TMEM161B-AS1 may play a role in GBM by modulating DNA damage repair-related genes and pathways, as indicated by KEGG pathway analysis. Specifically, our findings highlight the significance of the nucleotide excision repair and Fanconi anaemia (FA) pathway in the regulation of TMEM161B-AS1-regulated genes during the progression of GBM. Furthermore, Gene Ontology (GO) analysis demonstrated that TMEM161B-AS1-regulated genes are significantly enriched in biological processes associated with DNA replication and repair, as well as the cellular response to DNA damage stimuli. The complex interplay between DNA damage repair mechanisms and glioblastoma multiforme (GBM) is recognized as a critical determinant in the initiation, progression, and therapeutic resistance of these tumors. Studies have indicated that gliomas,

especially in individuals younger than 50 years, may be associated with Lynch syndrome due to deficiencies in mismatch repair mechanisms [29]. The involvement of UBE2M and its associated cullin ligases in glioma pathogenesis is significant, as they impact the cellular response to DNA damage [29]. The FA signaling pathway is essential for preserving genome integrity through the repair of DNA interstrand crosslinks that hinder replication and transcription processes. Its significance in cancer, particularly in glioma, is attributed to its ability to regulate DNA damage and prevent genomic instability, a key feature in cancer progression. The FA pathway has been identified as a critical mechanism in maintaining genome stability in response to various stressors, with mutations in FA genes contributing to genomic fragility and tumorigenesis [30]. Furthermore, the intricate architecture of the FA core complex and its interactions with various DNA repair proteins underscore the complex regulation of FA proteins in response to DNA damage, underscoring their significance in managing replication stress and safeguarding newly synthesized DNA strands [31]. Moreover, recent progress in elucidating the FA tumor suppressor pathway has provided insight into the crosstalk between FA proteins and alternative DNA repair pathways, such as the Rad6/Rad18 pathway, thereby highlighting the pivotal role of the FA pathway in the realm of cancer biology and therapeutic intervention [32]. The study conducted by Chen et al. elucidates the role of the Fanconi Anemia (FA) pathway in glioblastoma multiforme (GBM). Their findings suggest that downregulation of the Fanconi anemia complementation group D2 (FANCD2), a pivotal gene within the FA pathway, mediated by the knockdown of TMEM161B-AS1, is associated with ferroptosis and increased sensitivity to temozolomide (TMZ) in U87 and U251 cell lines [20]. This comprehensive understanding of the TMEM161B-AS1 regulated-pathways' function in DNA repair and its dysregulation in cancers like glioma underscores the potential for developing targeted therapies that exploit these mechanisms for cancer treatment.

Through the construction of a PPI network, three hub genes regulated by TMEM161B-AS1 were identified. These genes have been extensively linked to DNA damage repair or response and are implicated in the pathogenesis of GBM. Notably, the BRCA1 gene, which encodes the breast cancer type 1 susceptibility protein, also known as FANCJ (the gene mutated in the J complementation group of Fanconi anemia), plays a crucial role in DNA damage and repair processes, Fanconi anemia, and the development of various cancer types [33]. Furthermore, pan-cancer analyses utilizing public databases and a series of bioinformatic approaches have highlighted the involvement of BRIP1 in key biological pathways such as basal transcription factors, homologous recombination, and nucleotide excision repair. Significantly, there was a negative correlation observed between BRIP1 expression and DNA methylation levels in various tumors, suggesting its involvement in genetic regulation and possible influence on cancer cell behavior [33, 34]. Furthermore, CUL4A, a component of the ubiquitin ligase in the ubiquitin-proteasome system, is implicated in the degradation of proteins associated with the DNA damage response [35]. In GBM, Cullin 4A plays a crucial role in cancer progression by destabilizing the LATS1 protein through mediated ubiquitination, ultimately inhibiting the Hippo signaling pathway. This process promotes cell proliferation, invasion, and migration in glioma, emphasizing the involvement of S-100 Calcium Binding Protein A16 and underscoring the critical role of CUL4A in glioma development [35]. RPA1 (Replication protein 1) has been identified as a gene associated with DNA damage repair, which can be used as a prognostic marker for glioma and has a strong correlation with progression-free survival in pleomorphic xanthoastrocytoma patients [36]. In U87 cells subjected to a 7-day treatment with temozolomide (TMZ), quantitative proteomic analysis identified an enrichment of pathways related to DNA damage repair, notably involving the protein RPA1. RPA1 is a component of the Replication Protein A (RPA) complex, which is integral to the radio-resistance observed in glioma stem cells (GSCs). The expression of RPA is preferentially elevated in GSCs and correlates with unfavorable survival outcomes in patients with glioma. Interventions targeting RPA, either by downregulating its expression or through chemical inhibition, have been demonstrated to markedly reduce the survival and self-renewal capacities of GSCs, while concurrently increasing their vulnerability to ionizing radiation. These findings highlight the potential of RPA as a promising therapeutic target for the management of glioblastoma [37]. Therefore,

the involvement of lncRNA TMEM161B-AS1 and its regulated genes CUL4A, RPA1, and BRIP1 in glioblastoma further supports their potential as targets for therapeutic intervention and as biomarkers for disease progression or treatment response.

Our analysis also points to a possible functional interplay among the three hub genes we identified. CUL4A, RPA1, and BRIP1 each contribute to genomic stability through different but related mechanisms: CUL4A works through ubiquitin-mediated protein degradation, RPA1 helps stabilize replication forks, and BRIP1 handles interstrand crosslink repair. It is possible that TMEM161B-AS1 may disrupt these DNA damage response components in a coordinated way, setting up conditions that allow genomic instability to build up and push GBM progression forward. Looking at TMEM161B-AS1 regulation from this angle helps explain how one lncRNA can drive broad oncogenic effects by disturbing multiple DNA repair pathways at once.

Our study explored the complexity of glioma pathogenesis through the lens of lncRNAs. Our findings suggested that TMEM161B-AS1 may play a pivotal role in the pathogenesis of GBM and could serve as a therapeutic target for GBM patients. However, further research is necessary to clarify the role of TMEM161B-AS1 in GBM staging and its influence on disease progression. This study has several limitations. The meta-analysis of differentially expressed lncRNAs was based on data from diverse datasets, resulting in heterogeneity due to variations in sample sources, measurement techniques, and analytical tools. The breadth of sample coverage also affected the generalizability of our findings. Additionally, the study's predictions regarding the functions of lncRNAs and their regulatory genes were derived solely from analyses of public database data, underscoring a need for further validation through *in vitro* experiments and cell function verification. Thirdly, the identification of disease-relevant features from a large pool of genes was essential for enhancing the accuracy and interpretability of models, a task complicated by the sparse nature of the data and the limitations inherent in current methodologies.

Conclusion

This study aimed to investigate the expression profiles of lncRNAs in GBM using RNA sequencing analysis. Mendelian randomization analyses were employed to identify lncRNA TMEM-161B-AS1 was identified as a potential biomarker, with the aid of public databases for functional prediction. Three hub genes, CUL4A, RPA1, and BRIP1, were identified as being regulated by TMEM161B-AS1. Enrichment analysis revealed their involvement in glioma pathogenesis, particularly through the regulation of biologic processes such as DNA damage repair. This study offers insights into the molecular mechanisms of GBM development and establishes a theoretical foundation for potential therapeutic interventions for GBM, drug development, and personalized treatment approaches for GBM.

Acknowledgements

This work was supported by the Natural Science Foundation of Mongolia (Grant numbers 2024MS08042) and the Doctoral Projectof the First Hospital of Hohhot (Grant numbers 2023SYY(BS)016). The author thanks engineer Zhi-Hui Mi and Li-Na Chai of Inner Inner Mongolia Di An Feng Xin Medical Technology Co., LTD. for pro-viding data analysis services.

Disclosure of conflict of interest

None.

Address correspondence to: Shi-Chao Wang, The Clinical Genetic Laboratory, The First Hospital of Hohhot, No. 150, South Second Ring Road, Yuquan District, Hohhot 010018, Inner Mongolia Autonomous Region, China. E-mail: wscwawj2002@126.com

References

[1] Ostrom QT, Bauchet L, Davis FG, Deltour I, Fisher JL, Langer CE, Pekmezci M, Schwartzbaum JA, Turner MC, Walsh KM, Wrensch MR and Barnholtz-Sloan JS. The epidemiology of glioma in adults: a "state of the science" review. Neuro Oncol 2014; 16: 896-913.

[2] Thakkar JP, Dolecek TA, Horbinski C, Ostrom QT, Lightner DD, Barnholtz-Sloan JS and Villano JL. Epidemiologic and molecular prognostic review of glioblastoma. Cancer Epidemiol Biomarkers Prev 2014; 23: 1985-1996.

[3] Gondi V. Radiotherapy intensification for glioblastoma: enhancing the backbone of treatment. Chin Clin Oncol 2021; 10: 39.

[4] Molinaro AM, Taylor JW, Wiencke JK and Wrensch MR. Genetic and molecular epidemi-

ology of adult diffuse glioma. Nat Rev Neurol 2019; 15: 405-417.
[5] Liu B, Zhou J, Wang C, Chi Y, Wei Q, Fu Z, Lian C, Huang Q, Liao C, Yang Z, Zeng H, Xu N and Guo H. LncRNA SOX2OT promotes temozolomide resistance by elevating SOX2 expression via ALKBH5-mediated epigenetic regulation in glioblastoma. Cell Death Dis 2020; 11: 384.
[6] Liu P, Huang X, Wu H, Yin G and Shen L. LncRNA-H19 gene plays a significant role in regulating glioma cell function. Mol Genet Genomic Med 2021; 9: e1480.
[7] Katsushima K and Kondo Y. Non-coding RNAs as epigenetic regulator of glioma stem-like cell differentiation. Front Genet 2014; 5: 14.
[8] Jing SY, Lu YY, Yang JK, Deng WY, Zhou Q and Jiao BH. Expression of long non-coding RNA CRNDE in glioma and its correlation with tumor progression and patient survival. Eur Rev Med Pharmacol Sci 2016; 20: 3992-3996.
[9] He Y, Ye Y, Tian W and Qiu H. A novel lncRNA panel related to ferroptosis, tumor progression, and microenvironment is a robust prognostic indicator for glioma patients. Front Cell Dev Biol 2021; 9: 788451.
[10] Fernandez-Jimenez N and Bilbao JR. Mendelian randomization analysis of celiac GWAS reveals a blood expression signature with diagnostic potential in absence of gluten consumption. Hum Mol Genet 2019; 28: 3037-3042.
[11] Jiang T, Mao Y, Ma W, Mao Q, You Y, Yang X, Jiang C, Kang C, Li X, Chen L, Qiu X, Wang W, Li W, Yao Y, Li S, Li S, Wu A, Sai K, Bai H, Li G, Chen B, Yao K, Wei X, Liu X, Zhang Z, Dai Y, Lv S, Wang L, Lin Z, Dong J, Xu G, Ma X, Cai J, Zhang W, Wang H, Chen L, Zhang C, Yang P, Yan W, Liu Z, Hu H, Chen J, Liu Y, Yang Y, Wang Z, Wang Z, Wang Y, You G, Han L, Bao Z, Liu Y, Wang Y, Fan X, Liu S, Liu X, Wang Y and Wang Q; Chinese Glioma Cooperative Group (CGCG). CGCG clinical practice guidelines for the management of adult diffuse gliomas. Cancer Lett 2016; 375: 263-273.
[12] Paner GP, Stadler WM, Hansel DE, Montironi R, Lin DW and Amin MB. Updates in the eighth edition of the tumor-node-metastasis staging classification for urologic cancers. Eur Urol 2018; 73: 560-569.
[13] Xu S, Li X, Zhang S, Qi C, Zhang Z, Ma R, Xiang L, Chen L, Zhu Y, Tang C, Bourgonje AR, Li M, He Y, Zeng Z, Hu S, Feng R and Chen M. Oxidative stress gene expression, DNA methylation, and gut microbiota interaction trigger Crohn's disease: a multi-omics Mendelian randomization study. BMC Med 2023; 21: 179.
[14] GTEx Consortium. Human genomics. The Genotype-Tissue Expression (GTEx) pilot analysis: multitissue gene regulation in humans. Science 2015; 348: 648-660.
[15] Bowden J, Del Greco MF, Minelli C, Davey Smith G, Sheehan N and Thompson J. A framework for the investigation of pleiotropy in two-sample summary data Mendelian randomization. Stat Med 2017; 36: 1783-1802.
[16] Greco MF, Minelli C, Sheehan NA and Thompson JR. Detecting pleiotropy in Mendelian randomisation studies with summary data and a continuous outcome. Stat Med 2015; 34: 2926-2940.
[17] Li JH, Liu S, Zhou H, Qu LH and Yang JH. starBase v2.0: decoding miRNA-ceRNA, miRNA-ncRNA and protein-RNA interaction networks from large-scale CLIP-Seq data. Nucleic Acids Res 2014; 42: D92-97.
[18] Szklarczyk D, Franceschini A, Wyder S, Forslund K, Heller D, Huerta-Cepas J, Simonovic M, Roth A, Santos A, Tsafou KP, Kuhn M, Bork P, Jensen LJ and von Mering C. STRING v10: protein-protein interaction networks, integrated over the tree of life. Nucleic Acids Res 2015; 43: D447-452.
[19] Xie R, Li B, Jia L and Li Y. Identification of core genes and pathways in melanoma metastasis via bioinformatics analysis. Int J Mol Sci 2022; 23: 794.
[20] Chen Q, Wang W, Wu Z, Chen S, Chen X, Zhuang S, Song G, Lv Y and Lin Y. Over-expression of lncRNA TMEM161B-AS1 promotes the malignant biological behavior of glioma cells and the resistance to temozolomide via up-regulating the expression of multiple ferroptosis-related genes by sponging hsa-miR-27a-3p. Cell Death Discov 2021; 7: 311.
[21] Ling H, Vincent K, Pichler M, Fodde R, Berindan-Neagoe I, Slack FJ and Calin GA. Junk DNA and the long non-coding RNA twist in cancer genetics. Oncogene 2015; 34: 5003-5011.
[22] Hou XR, Zhang ZD, Cao XL and Wang XP. Long noncoding RNAs, glucose metabolism and cancer (Review). Oncol Lett 2023; 26: 340.
[23] Shi Z, Li G, Li Z, Liu J and Tang Y. TMEM161B-AS1 suppresses proliferation, invasion and glycolysis by targeting miR-23a-3p/HIF1AN signal axis in oesophageal squamous cell carcinoma. J Cell Mol Med 2021; 25: 6535-6549.
[24] Wang M, Han Z, Wang X, Cheng Y, Cao Z, Zhang Y and Zhang Y. lncRNA TMEM161B-AS1 screened the onset of oral squamous cell carcinoma in HPV-infected patients, predicted poor prognosis, and regulated cell progression via modulating the miR-651-5p/BDNF axis. Odontology 2024; 112: 1010-1022.
[25] Zeng T, Jiang S, Wang Y, Sun G, Cao J, Hu D, Wang G, Liang X, Ding J and Du J. Identification and validation of a cellular senescence-related lncRNA signature for prognostic prediction in patients with multiple myeloma. Cell Cycle 2023; 22: 1434-1449.

[26] Luo P, Yang J, Jian L, Dong J, Yin S, Luo C and Zhou S. Knockdown of PGBD5 inhibits the malignant progression of glioma through upregulation of the PPAR pathway. Int J Oncol 2024; 64: 55.
[27] Yan C, Yang Z, Chen P, Yeh Y, Sun C, Xie T, Huang W and Zhang X. GPR65 sensing tumor-derived lactate induces HMGB1 release from TAM via the cAMP/PKA/CREB pathway to promote glioma progression. J Exp Clin Cancer Res 2024; 43: 105.
[28] Orda MA, Fowler PMPT and Tayo LL. Modular hub genes in DNA microarray suggest potential signaling pathway interconnectivity in various glioma grades. Biology (Basel) 2024; 13: 206.
[29] Cukras S, Morffy N, Ohn T and Kee Y. Inactivating UBE2M impacts the DNA damage response and genome integrity involving multiple cullin ligases. PLoS One 2014; 9: e101844.
[30] Badra Fajardo N, Taraviras S and Lygerou Z. Fanconi anemia proteins and genome fragility: unraveling replication defects for cancer therapy. Trends Cancer 2022; 8: 467-481.
[31] Niraj J, Farkkila A and D'Andrea AD. The Fanconi anemia pathway in cancer. Annu Rev Cancer Biol 2019; 3: 457-478.
[32] Pickering A, Zhang J, Panneerselvam J and Fei P. Advances in the understanding of the Fanconi anemia tumor suppressor pathway. Cancer Biol Ther 2013; 14: 1089-1091.
[33] Wang R, Zhang J, Cui X, Wang S, Chen T, Niu Y, Du X, Kong J, Wang L and Jiang Y. Multimolecular characteristics and role of BRCA1 interacting protein C-terminal helicase 1 (BRIP1) in human tumors: a pan-cancer analysis. World J Surg Oncol 2023; 21: 91.
[34] Liu Y, Wu X, Feng Y, Jiang Q, Zhang S, Wang Q and Yang A. Insights into the oncogenic, prognostic, and immunological role of BRIP1 in pan-cancer: a comprehensive data-mining-based study. J Oncol 2023; 2023: 4104639.
[35] Hu Y, Zhang R, Lu S, Zhang W, Wang D, Ge Y, Jiang F, Qin X and Liu Y. S100 Calcium Binding Protein A16 Promotes Cell Proliferation by triggering LATS1 ubiquitin degradation mediated by CUL4A ligase to inhibit Hippo pathway in Glioma development. Int J Biol Sci 2023 19: 2034-2052.
[36] Dandapath I, Gupta R, Singh J, Shukla N, Jha P, Sharma V, Suri A, Sharma MC, Suri V, Sarkar C and Kulshreshtha R. Long non-coding RNA and mRNA Co-expression network reveals novel players in pleomorphic xanthoastrocytoma. Mol Neurobiol 2022; 59: 5149-5167.
[37] Pedersen H, Obara EAA, Elbæk KJ, Vitting-Serup K and Hamerlik P. Replication protein A (RPA) mediates radio-resistance of glioblastoma cancer stem-like cells. Int J Mol Sci 2020; 21: 1588.

Table S1. DE lncRNAs

LncRNA	Log_2FC	FDR	Style	Location	Strand
ENSG00000185837.3	Inf	0.005694	Up	chr22_2217159384_17165439	+
ENSG00000228463.9	Inf	0.017627	Up	chr1_266361_297502	-
ENSG00000185837.3	3.30158	0.03762	Up	chr22_17159399_17165445	+
ENSG00000235366.2	5.780278	0.019621	Up	chr13_45680184_45701184	-
ENSG00000235897.1	Inf	0.03037	Up	chr3_196318406_196324188	+
ENSG00000228315.11	3.386296	0.002744	Up	chr22_23638487_23693151	-
ENSG00000240875.5	Inf	0.039771	Up	chr3_156750001_156751519	-
ENSG00000240057.5	3.256939	0.01952	Up	chr3_113019533_113088715	+
ENSG00000249307.5	5.052585	0.005493	Up	chr4_79258781_79308654	+
ENSG00000249307.5	2.361099	0.030368	Up	chr4_79211681_79245532	+
ENSG00000249307.5	2.808152	0.016659	Up	chr4_79305123_79308798	+
ENSG00000214548.14	Inf	0.020493	Up	chr14_100832969_100861021	+
ENSG00000260391.2	3.930152	0.006726	Up	chr3_124723788_124726325	+
XLOC_019040	Inf	0.010122	Up	chr1_84613815_84621009	-
XLOC_019813	Inf	0.027765	Up	chr1_90374003_90420449	-
XLOC_020592	Inf	0.023653	Up	chr1_109514704_109522694	-
XLOC_033405	Inf	0.027822	Up	chr10_87458626_87492424	+
XLOC_040050	3.341487	0.038722	Up	chr10_83914363_84049305	-
XLOC_045043	Inf	0.017004	Up	chr11_33835699_33858667	+
XLOC_056010	Inf	0.006839	Up	chr11_82796934_82797488	-
XLOC_078789	3.132943	0.024325	Up	chr13_77850775_77914632	+
XLOC_080147	2.80786	0.043285	Up	chr13_95300922_95312194	+
XLOC_115160	Inf	0.03034	Up	chr16_18052155_18136580	-
XLOC_125784	3.826649	0.023139	Up	chr17_38244499_38245567	+
XLOC_131364	3.734489	0.040925	Up	chr18_35356231_35356983	+
XLOC_161705	5.747195	0.022992	Up	chr2_241820100_241822181	+
XLOC_164705	11.74011	0.005645	Up	chr2_32916213_32916618	-
XLOC_164705	Inf	0.010249	Up		
XLOC_168953	Inf	0.036278	Up	chr2_92188172_92237317	-
XLOC_168978	Inf	0.01441	Up	chr2_92728335_92787741	-
XLOC_169062	4.664016	0.045734	Up	chr2_93357369_93385636	-
XLOC_169112	Inf	0.02842	Up	chr2_94140558_94156747	-
XLOC_198663	Inf	0.000301	Up	chr3_83953614_84059477	+
XLOC_202277	Inf	0.037008	Up	chr3_153185507_153185929	+
XLOC_210683	Inf	0.037318	Up	chr3_123588122_123589341	-
XLOC_219310	2.152807	0.041188	Up	chr4_79202814_79204855	+
XLOC_228781	Inf	2.33E-05	Up	chr4_47027706_47032749	-
XLOC_247874	3.651653	0.030167	Up	chr5_172013844_172020562	+
XLOC_249865	Inf	0.044745	Up	chr5_15425332_15425876	-
XLOC_259353	Inf	0.018348	Up	chr5_162534929_162539068	-
XLOC_265610	4.778952	0.009191	Up	chr6_71238550_71240003	+
XLOC_268753	Inf	0.009208	Up	chr6_111686228_111697853	+
XLOC_272726	4.485256	0.025239	Up	chr6_164927808_164931121	+
XLOC_276571	Inf	0.014933	Up	chr6_35257081_35259551	-
XLOC_277968	Inf	0.01983	Up	chr6_70384015_70388061	-
XLOC_288937	Inf	0.024828	Up	chr7_67357774_67360681	+
XLOC_302093	Inf	0.003595	Up	chr7_130319041_130331970	-

XLOC_303175	Inf	0.003122	Up	chr7_149993153_150012322	-
XLOC_311294	Inf	0.03206	Up	chr8_117245273_117248081	+
XLOC_317217	4.089205	0.012542	Up	chr8_66198930_66221103	-
XLOC_325487	Inf	0.032466	Up	chr9_61892946_61895741	+
XLOC_332734	6.376727	0.011558	Up	chr9_26346244_26569677	
ENSG00000174403.15	-2.7012	0.031411	Down	chr20_62544343_62551526	-
ENSG00000229588.1	Inf	0.043235	Down	chr1_166334884_166335762	+
ENSG00000237737.5	-4.06678	0.002733	Down	chr2_74385497_74391904	+
ENSG00000243701.5	-4.30416	0.03242	Down	chr3_107240692_107326964	+
ENSG00000205930.8	Inf	0.03869	Down	chr21_32772161_32852470	+
ENSG00000248455.5	-4.38593	0.049939	Down	chr21_32772100_32798969	+
ENSG00000247828.7	-2.70681	0.020203	Down	chr5_88268916_88436685	+
ENSG00000245146.6	Inf	0.031289	Down	chr5_140102922_140107643	-
ENSG00000256193.5	-5.94665	0.022486	Down	chr12_127915372_127951510	+
ENSG00000262223.6	Inf	0.003783	Down	chr17_81376001_81385360	-
ENSG00000263069.5	Inf	0.028468	Down	chr17_80351828_80415118	-
ENSG00000263766.5	-3.95284	0.017324	Down	chr17_47603860_47649402	-
ENSG00000186594.12	Inf	0.001059	Down	chr17_1712825_1716209	-
ENSG00000228794.8	-5.16525	0.010188	Down	chr1_827608_859446	+
XLOC_000367	-6.26283	0.031884	Down	GL000219.1_49899_51093	-
XLOC_000434	Inf	0.038025	Down	GL000225.1_6792_34488	-
XLOC_000839	Inf	0.01673	Down	KI270733.1_133088_135658	+
XLOC_007755	Inf	0.021498	Down	chr1_121611037_121614637	+
XLOC_032710	Inf	0.021326	Down	chr10_71829031_71851259	+
XLOC_037210	Inf	0.045953	Down	chr10_21251732_21293035	-
XLOC_037967	Inf	0.04384	Down	chr10_42235500_42237100	-
XLOC_039296	-6.90085	0.013361	Down	chr10_69088142_69104801	-
XLOC_040623	-3.2349	0.042694	Down	chr10_93755849_93757731	-
XLOC_045448	Inf	0.047729	Down	chr11_46777503_46778510	+
XLOC_060487	Inf	0.004371	Down	chr12_14942033_14961587	+
XLOC_073979	Inf	0.045961	Down	chr12_109624045_109625145	-
XLOC_116066	-3.24394	0.033192	Down	chr16_51379750_51525103	-
XLOC_122620	-7.16795	0.022717	Down	chr17_58269854_58280897	+
XLOC_124776	Inf	0.001216	Down	chr17_17033378_17040121	-
XLOC_129378	Inf	0.029025	Down	chr17_81703493_81707232	-
XLOC_141586	Inf	0.00059	Down	chr19_48493613_48498107	+
XLOC_164705	Inf	0.002668	Down	chr2_32916213_32916618	-
XLOC_164705	-6.08031	0.042932	Down		
XLOC_169093	Inf	0.024453	Down	chr2_93768431_93810587	-
XLOC_169575	Inf	0.020923	Down	chr_103449784_103480540	-
XLOC_189417	Inf	0.026241	Down	chr22_19291923_19333973	+
XLOC_196104	Inf	0.045259	Down	chr3_33883741_33886889	+
XLOC_196947	Inf	0.040958	Down	chr3_47062163_47083824	+
XLOC_211305	-6.26792	0.004193	Down	chr3_133746414_133778740	-
XLOC_223733	Inf	0.047406	Down	chr4_154604330_154609741	+
XLOC_228769	Inf	0.010921	Down	chr4_45957711_45958878	-
XLOC_229641	Inf	0.014756	Down	chr4_73436238_73450754	-
XLOC_229642	Inf	0.041203	Down	chr4_73452428_73455745	-
XLOC_230383	Inf	0.038664	Down	chr4_87806174_87811756	-

XLOC_240626	Inf	0.009353	Down	chr5_88804619_88823816	+
XLOC_243325	Inf	0.021126	Down	chr5_117262803_117309155	+
XLOC_260368	Inf	0.033685	Down	chr5_176731971_176732662	-
XLOC_282244	Inf	0.039356	Down	chr6_132814586_132817540	-
XLOC_296063	Inf	0.010965	Down	chr7_23035087_23042111	-
XLOC_303273	Inf	0.044795	Down	chr7_150221282_150238110	-
XLOC_325487	Inf	0.029909	Down	chr9_61892946_61895741	+
XLOC_345209	-4.90075	0.001472	Down	chrX_115726219_115737393	+
XLOC_345209	-7.74281	6.20E-05	Down	chrX_115726269_115737393	+
XLOC_357378	Inf	0.024658	Down	chrY_20067446_20075411	+

Table S2. MR analysis

Exposure	LncRNA-Symbol	Outcome	Method	Nsnp	Beta	SE	Pval	LCI	UCI
ENSG00000228315.11	GUSBP11	Brain glioblastoma	MR Egger	9	1.3577392	0.5092175	0.0321707	0.3596729	2.3558055
ENSG00000228315.11	GUSBP11	Brain glioblastoma	Weighted median	9	0.4197997	0.1634852	0.0102342	0.0993687	0.7402306
ENSG00000228315.11	GUSBP11	Brain glioblastoma	Inverse variance weighted	9	0.2390697	0.1155895	0.0586151	-0.012514	0.4656252
ENSG00000228315.11	GUSBP11	Brain glioblastoma	Simple mode	9	0.4658087	0.2366927	0.0846063	0.0018911	0.9297264
ENSG00000228315.11	GUSBP11	Brain glioblastoma	Weighted mode	9	0.4658087	0.2606916	0.111781	-0.045147	0.9767642
ENSG00000249307.5	LINC01088	Brain glioblastoma	MR Egger	21	0.5692829	0.3024728	0.0752317	-0.023564	1.1621295
ENSG00000249307.5	LINC01088	Brain glioblastoma	Weighted median	21	0.4471577	0.1087166	3.90E-05	0.2340731	0.6602424
ENSG00000249307.5	LINC01088	Brain glioblastoma	Inverse variance weighted	21	0.1256692	0.0808442	0.0524793	-0.067215	0.2541238
ENSG00000249307.5	LINC01088	Brain glioblastoma	Simple mode	21	0.4484914	0.1692396	0.0153651	0.1167818	0.7802011
ENSG00000249307.5	LINC01088	Brain glioblastoma	Weighted mode	21	0.4484914	0.1812	0.0223901	0.0933394	0.8036435
ENSG00000247828.7	TMEM161B-AS1	Brain glioblastoma	MR Egger	30	-0.183628	0.6975542	0.7942891	-1.550834	1.1835783
ENSG00000247828.7	TMEM161B-AS1	Brain glioblastoma	Weighted median	30	0.2976236	0.0687053	1.48E-05	0.1629612	0.4322861
ENSG00000247828.7	TMEM161B-AS1	Brain glioblastoma	Inverse variance weighted	30	0.2537691	0.0532382	1.87E-06	0.1494222	0.3581159
ENSG00000247828.7	TMEM161B-AS1	Brain glioblastoma	Simple mode	30	0.2781842	0.1215919	0.0296251	0.0398642	0.5165043
ENSG00000247828.7	TMEM161B-AS1	Brain glioblastoma	Weighted mode	30	0.2926554	0.1167565	0.0180502	0.0638126	0.5214982

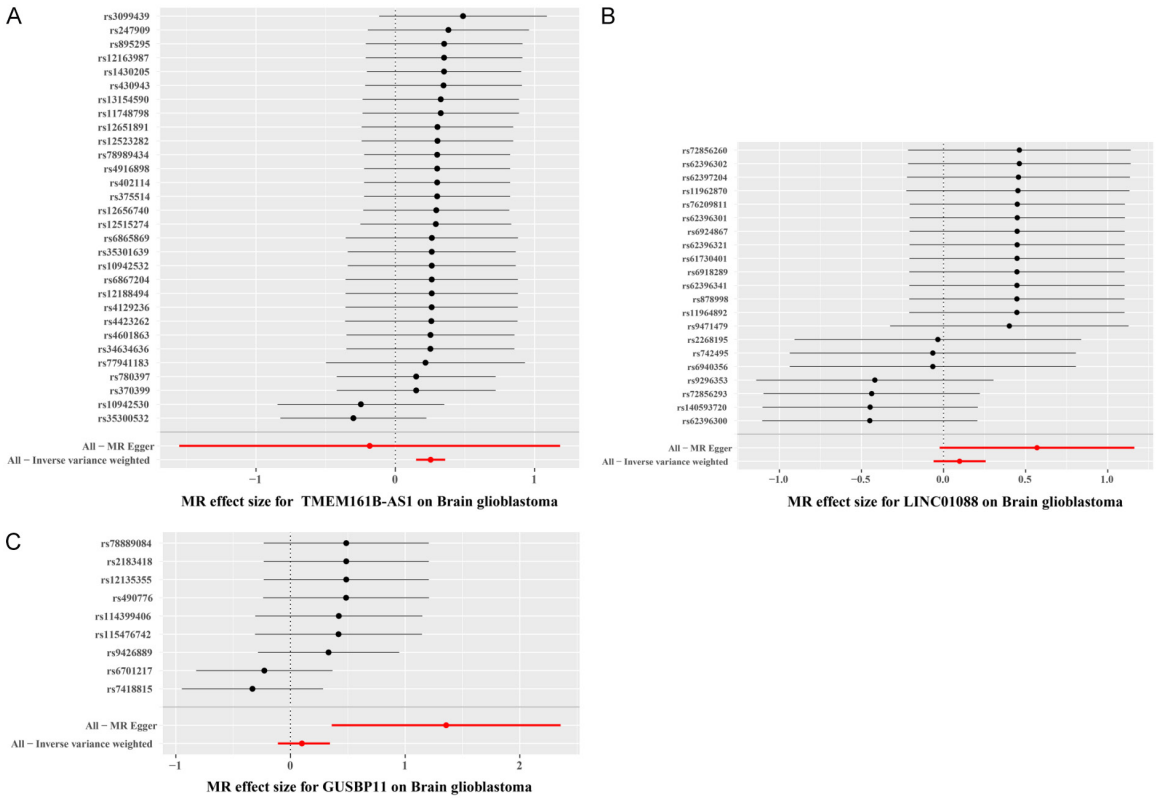

Figure S1. Forest plots of causal effects of DE-lncRNA related single nucleotide polymorphisms on GBM. A. TMEM161B-AS1; B. LINC01088; C. GUSBP11.

Table S3. Heterogeneity tests of MR

Exposure	LncRNA-Symbol	Outcome	method	Q	Q_df	Q_pval
ENSG00000228315.11	GUSBP11	Brain glioblastoma	MR Egger	20.76168	19	0.3501175
ENSG00000228315.11	GUSBP11	Brain glioblastoma	Inverse variance weighted	22.27814	20	0.3256108
ENSG00000249307.5	LINC01088	Brain glioblastoma	MR Egger	8.126081	8	0.4212521
ENSG00000249307.5	LINC01088	Brain glioblastoma	Inverse variance weighted	0.1348124	9	0.5206196
ENSG00000247828.7	TMEM161B-AS1	Brain glioblastoma	MR Egger	31.398122	27	0.2551081
ENSG00000247828.8	TMEM161B-AS2	Brain glioblastoma	Inverse variance weighted	31.912654	28	0.27808

Table S4. Pleiotropy tests of MR

Exposure	LncRNA-Symbol	Outcome	Egger_intercept	Se	Pval
ENSG00000228315.11	GUSBP11	Brain glioblastoma	-0.226098596	0.1919273	0.2533245
ENSG00000249307.5	LINC01088	Brain glioblastoma	0.194550142	2.0820437	0.9278503
ENSG00000247828.7	TMEM161B-AS1	Brain glioblastoma	0.254674098	0.4049658	0.5345262

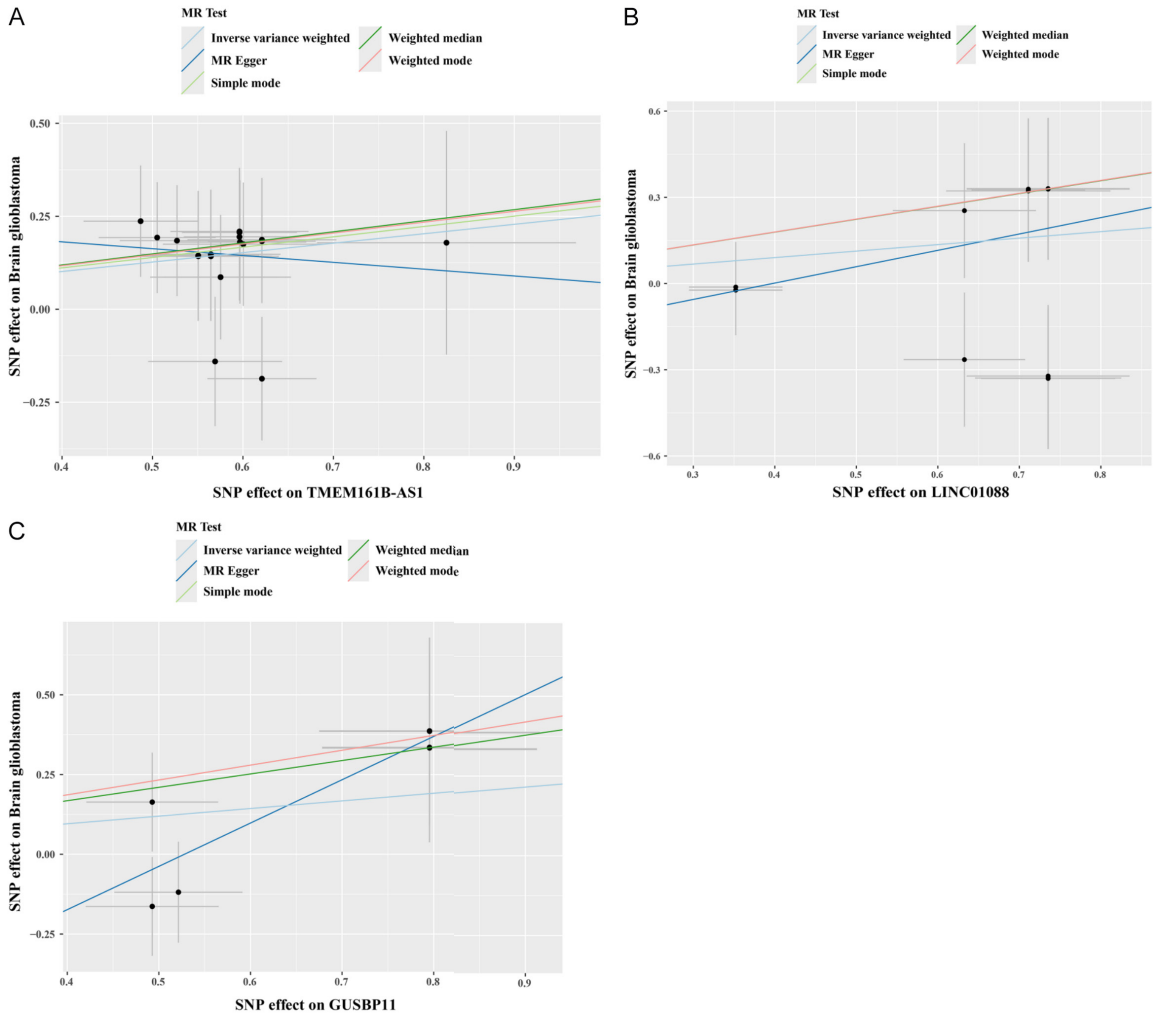

Figure S2. Scatter plots of genetic association between DE-lncRNA and GBM. A. TMEM161B-AS1; B. LINC01088; C. GUSBP11.

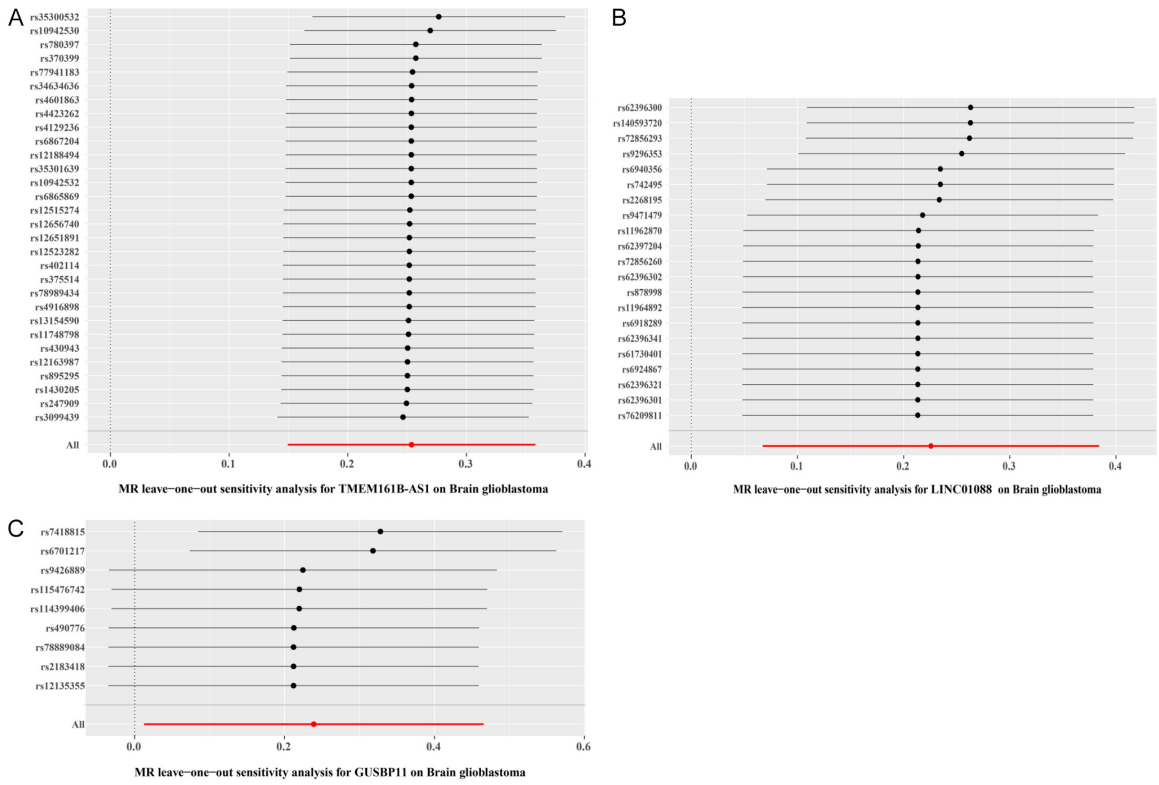

Figure S3. Forest plots of Leave-one-out analyses. A. TMEM161B-AS1; B. LINC01088; C. GUSBP11.

Table S5. mRNAs regulated by TMEM161B-AS1

Gene ID	Gene Name	Free Energy	Align Score (Smith-Waterman)
ENSG00000038382	TRIO	-33.3	21.5
ENSG00000049192	ADAMTS6	-22.8	14
ENSG00000052126	PLEKHA5	-17.3	14
ENSG00000072364	AFF4	-22.7	17
ENSG00000075391	RASAL2	-21.3	19.5
ENSG00000076706	MCAM	-33.5	16
ENSG00000078304	PPP2R5C	-17.9	12.5
ENSG00000079950	STX7	-25.1	21
ENSG00000092203	TOX4	-17	13
ENSG00000099194	SCD	-25.9	17
ENSG00000100345	MYH9	-15.2	14
ENSG00000102471	NDFIP2	-18.8	20
ENSG00000103942	HOMER2	-31.1	20
ENSG00000104824	HNRNPL	-18.9	23.5
ENSG00000105887	MTPN	-23.2	19
ENSG00000107745	MICU1	-33.9	25
ENSG00000107862	GBF1	-22.1	11
ENSG00000109184	DCUN1D4	-38.8	13
ENSG00000111700	SLCO1B3	-17.9	22.5
ENSG00000112541	PDE10A	-25.3	22.5
ENSG00000112941	TENT4A	-27.2	13.5
ENSG00000113273	ARSB	-16.6	18

ENSG00000113448	PDE4D	-29.8	17
ENSG00000115306	SPTBN1	-32.6	23
ENSG00000115365	LANCL1	-48.7	34
ENSG00000116729	WLS	-26.8	17
ENSG00000122008	POLK	-25.7	27
ENSG00000132383	RPA1	-23.4	20
ENSG00000132463	GRSF1	-16.4	12.5
ENSG00000134480	CCNH	-21.5	16.5
ENSG00000134909	ARHGAP32	-16	12.5
ENSG00000136068	FLNB	-27.2	19
ENSG00000139842	CUL4A	-16.3	19.5
ENSG00000140577	CRTC3	-27.1	15
ENSG00000145545	SRD5A1	-22.9	17.5
ENSG00000147202	DIAPH2	-32.3	19
ENSG00000151914	DST	-19.7	26
ENSG00000153250	RBMS1	-26.4	10
ENSG00000153815	CMIP	-17.2	14
ENSG00000153944	MSI2	-41.9	20
ENSG00000155034	FBXL18	-27.8	10
ENSG00000155111	CDK19	-18.8	20
ENSG00000160563	MED27	-22.3	10
ENSG00000163930	BAP1	-42.7	29.5
ENSG00000164073	MFSD8	-19.8	14
ENSG00000164176	EDIL3	-43.1	23
ENSG00000164180	TMEM161B	-23.1	24
ENSG00000166833	NAV2	-33.4	10
ENSG00000171435	KSR2	-22.7	14
ENSG00000171444	MCC	-23.9	22.5
ENSG00000172572	PDE3A	-25	11.5
ENSG00000173744	AGFG1	-38	24.5
ENSG00000180104	EXOC3	-39.6	45
ENSG00000181722	ZBTB20	-23.5	16
ENSG00000182310	SPACA6	-25.9	14
ENSG00000184349	EFNA5	-23.9	15
ENSG00000186314	PRELID2	-41.3	14.5
ENSG00000186350	RXRA	-39.4	20
ENSG00000196600	SLC22A25	-17.6	17
ENSG00000197622	CDC42SE1	-36.4	29.5
ENSG00000198108	CHSY3	-22.7	20.5
ENSG00000198130	HIBCH	-36.7	19
ENSG00000204536	CCHCR1	-34.1	22
ENSG00000214113	LYRM4	-45.3	13
ENSG00000234602	MCIDAS	-15.6	13
ENSG00000005483	KMT2E	-25.6	24
ENSG00000011376	LARS2	-26.3	18
ENSG00000020577	SAMD4A	-34.2	19
ENSG00000049323	LTBP1	-18.7	15.5
ENSG00000052749	RRP12	-29	19.5
ENSG00000065135	GNAI3	-25.8	28

ENSG00000079819	EPB41L2	-32.7	26
ENSG00000082438	COBLL1	-17.8	13.5
ENSG00000083123	BCKDHB	-30.1	19
ENSG00000100749	VRK1	-38.2	18
ENSG00000104626	ERI1	-29.8	15.5
ENSG00000106144	CASP2	-28	19
ENSG00000106682	EIF4H	-28.8	15.5
ENSG00000107669	ATE1	-17.7	13
ENSG00000109332	UBE2D3	-28.3	24
ENSG00000111817	DSE	-26.1	13.5
ENSG00000112319	EYA4	-16.6	12
ENSG00000113387	SUB1	-18.3	13.5
ENSG00000114439	BBX	-22.4	16.5
ENSG00000114541	FRMD4B	-34.7	17.5
ENSG00000115998	C2orf42	-27.2	12
ENSG00000116741	RGS2	-19.8	27.5
ENSG00000119314	PTBP3	-26.4	16
ENSG00000119844	AFTPH	-35.3	10
ENSG00000120647	CCDC77	-36.7	17
ENSG00000120658	ENOX1	-33.4	15.5
ENSG00000121542	SEC22A	-18.9	12.5
ENSG00000124225	PMEPA1	-18.3	19.5
ENSG00000125877	ITPA	-29.1	20
ENSG00000127481	UBR4	-28	22.5
ENSG00000128487	SPECC1	-18.4	18
ENSG00000132563	REEP2	-19.4	12
ENSG00000133393	CEP20	-73.1	53.5
ENSG00000134318	ROCK2	-22.2	20
ENSG00000134824	FADS2	-23.6	14
ENSG00000136492	BRIP1	-27.4	17.5
ENSG00000138375	SMARCAL1	-36.1	16
ENSG00000140948	ZCCHC14	-55	26
ENSG00000142875	PRKACB	-81.3	50.5
ENSG00000143164	DCAF6	-25.2	15.5
ENSG00000145555	MYO10	-59.8	54
ENSG00000145700	ANKRD31	-27.8	20.5
ENSG00000145734	BDP1	-26	12
ENSG00000147677	EIF3H	-42.7	11.5
ENSG00000151883	PARP8	-28	27.5
ENSG00000158545	ZC3H18	-26.6	16
ENSG00000161217	PCYT1A	-31.3	15.5
ENSG00000162415	ZSWIM5	-32.3	26.5
ENSG00000162599	NFIA	-19.7	13.5
ENSG00000165669	FAM204A	-27.9	12
ENSG00000167325	RRM1	-20.8	20
ENSG00000168175	MAPK1IP1L	-21.1	20
ENSG00000168615	ADAM9	-36.6	21
ENSG00000169752	NRG4	-42.2	20
ENSG00000173273	TNKS	-42.9	26

ENSG00000174989	FBXW8	-20.6	16
ENSG00000175073	VCPIP1	-28.2	18
ENSG00000175137	SH3BP5L	-19.6	16.5
ENSG00000181894	ZNF329	-33.5	14
ENSG00000184903	IMMP2L	-24.8	22
ENSG00000186566	GPATCH8	-18.8	16.5
ENSG00000187079	TEAD1	-31	21.5
ENSG00000197008	ZNF138	-32.4	16.5
ENSG00000197375	SLC22A5	-17.1	23.5
ENSG00000198677	TTC37	-22.7	14
ENSG00000198700	IPO9	-24.4	18
ENSG00000198732	SMOC1	-39.8	18.5
ENSG00000205323	SARNP	-29.7	22.5
ENSG00000214944	ARHGEF28	-19.6	16.5
ENSG00000215712	TMEM242	-27.6	17
ENSG00000229117	RPL41	-33.3	16
ENSG00000257727	CNPY2	-20.3	13.5